P2.5 TROPICAL PRECIPITATION PATTERNS IN RESPONSE TO A LOCAL WARM SST AREA PLACED AT THE EQUATOR OF AN AQUA PLANET: AN ENSEMBLE STUDY

Kensuke Nakajima *
Kyushu University, Fukuoka, Japan
Masaki Ishiwatari
Hokkaido University, Sapporo, Japan
Shin-ichi Takehiro
Kyushu University, Fukuoka, 812-8581, Japan
Eizi Toyoda
Japan Meteorological Agency, Tokyo, Japan
Yoshi-Yuki Hayashi
Hokkaido University, Sapporo, Japan

1. INTRODUCTION

The relationship between the inhomogeneities of the boundary conditions (e.g., SST) and the observed precipitation or circulation patterns is not necessarily straightforward because the amount of precipitation is affected not only directly by the in situ surface boundary conditions but also remotely by the circulations driven by the distant features (thermal and/or topographic forcing). With this issue in mind, Hosaka *et al.* (1998, hereafter, referred to as H98) investigated possible precipitation patterns over the entire tropical region with a simple "aqua planet" setup. In order to clarify idealistic remote effects of the active convection center on the distribution of precipitation over the entire tropical region, one localized warm SST anomaly is placed at the equator on a zonally and equatorially symmetric basic SST distribution.

Other than the convection center over the warm SST area, the statistically steady response obtained by H98 is characterized with the east-west asymmetric remote response. In an extensive region to the east of the warm SST area, precipitation is enhanced and pressure anomaly is negative. On the other hand, drying occurs and pressure rises to the west. The appearance of the high pressure anomaly to the west is particularly curious, since, according to the simple linear longwave theory of Gill (1980) or Heckley and Gill (1984), surface pressure anomaly should be negative both to the east and to the west of the convection center (heat source).

H98 presents a possible scenario for the appearance of the east-west asymmetries of remote response based on the equatorial wave dynamics and water vapor transport in surface Ekman layer. An initial switch-on experiment must be useful to verify the scenario. However, the initial development of the response is severely contaminated by two types of noise, which are the grid point moist convection event and eastward propagating moist Kelvin wave related to Madden–Julian Oscillation (MJO; Madden and Julian, 1972). H98 suggests that the ensemble averaging of a set of runs starting from different initial conditions may be useful in extracting the evolution of the response masked by those noises. Following this suggestion, Toyoda *et al.* (1999) conducted a preliminary ensemble experiment with the experimental set-up being the same as that of H98, and concluded that the evolution of large scale features can be satisfactory extracted by averaging 128 runs.

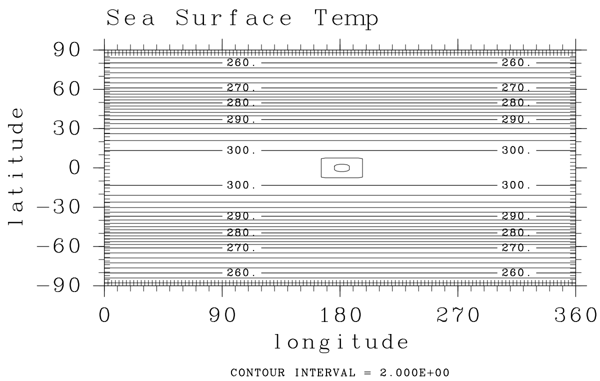

1: The distribution of SST utilized in the experiment. Contour interval in 2K, and unit is K.

The present study extend the ensemble experiment of Toyoda *et al.* (1999) and try to clarify the initial development of the response field after the switch-on of the warm SST anomaly. In particular, we try to verify the scenario proposed by H98 of the evolution of the east-west asymmetry caused by the convection center over the warm SST area. These information on the temporal evolution will be useful particularly when the practical application is concerned, since the real SST distribution often varies with the time scale which is not much longer than that of the adjustment to the steady state response.

2. EXPERIMENTAL DESIGN

The model used here is the simple T42L16 moist GCM used by H98. The ensemble experiment consists of 128 runs. Each run is integrated for 50 days, starting from a different initial condition with a common SST distribution

*Corresponding author address: Kensuke Nakajima, Faculty of Sciences, Kyushu University, Fukuoka, 812-8581, JAPAN; e-mail: kensuke@geo.kyushu-u.ac.jp

(Fig.1), which is the same as that for case A4 of H98. The peak value of the SST anomaly is 4K.

The initial conditions of the ensemble runs are sampled from the time series of an experiment without SST anomaly. In addition, a separate, long term integration with the SST anomaly, which is basically the same experiment as case A4 of H98, is performed for the sake of comparison between the ensemble and temporal averages. Other details are described in Toyoda *et al.*(2002).

Toyoda *et al.* (1999) defines the ensemble mean anomaly as the difference between an ensemble averaged field obtained from the runs with SST anomaly and the zonally and temporally averaged field of the run without SST anomaly. In the present study, we examine another definition of ensemble mean anomaly. Corresponding to each SST anomaly run, we have the SST anomaly-free run which started from the same initial condition as that of the SST anomaly run. Using these time series, we can calculate the difference between the ensemble averaged field of the runs with SST anomaly and the ensemble averaged field of the runs without SST anomaly. Hereafter, when we need to distinguish those two definition of ensemble mean anomaly, the definition by Toyoda *et al* (1999) is referred to as “ensemble mean anomaly from zonal and temporal average”, while that defined above is referred to as “ensemble mean anomaly from individual”.

3. EFFECTIVENESS OF ENSEMBLE AVERAGING IN NOISE REDUCTION

Before examining the time evolution of ensemble average of the atmospheric response to the introduction of the warm SST area, we briefly demonstrate the effectiveness of the ensemble experiment. Fig.2 (a) and (b) show the horizontal distributions of the precipitation anomaly at day 50 obtained by a single run and that by the average of 128 runs, respectively. The response obtained by a single run (Fig.2(a)) is characterized with a number of positive anomalies and zonally distributed negative anomalies. The positive anomalies correspond to moist convection activities associated with various transient disturbances such as super clusters along the equator, tropical cyclones along the ITCZs, and baroclinic waves in the extratropics. The zonally distributed negative anomalies are the reflections of the climatological precipitation zones, i.e., ITCZs and mid-latitude baroclinic zones. In all latitudinal bands, positive anomalies are so intense that the signatures caused by the SST anomaly, including the convection center itself, can be hardly recognized. In the response obtained by the 128 ensemble average (Fig.2(b))), the convection center appears quite prominently as the positive anomaly above the warm SST area. To the east of the convection center, positive precipitation anomaly prevails along the equator, while, to the west of the convection center, negative anomaly is evident. North-south symmetric mid-latitudes anomalies, which are presumably associated with the stationary planetary wave packets emitted from the convection center, can also be recognized.

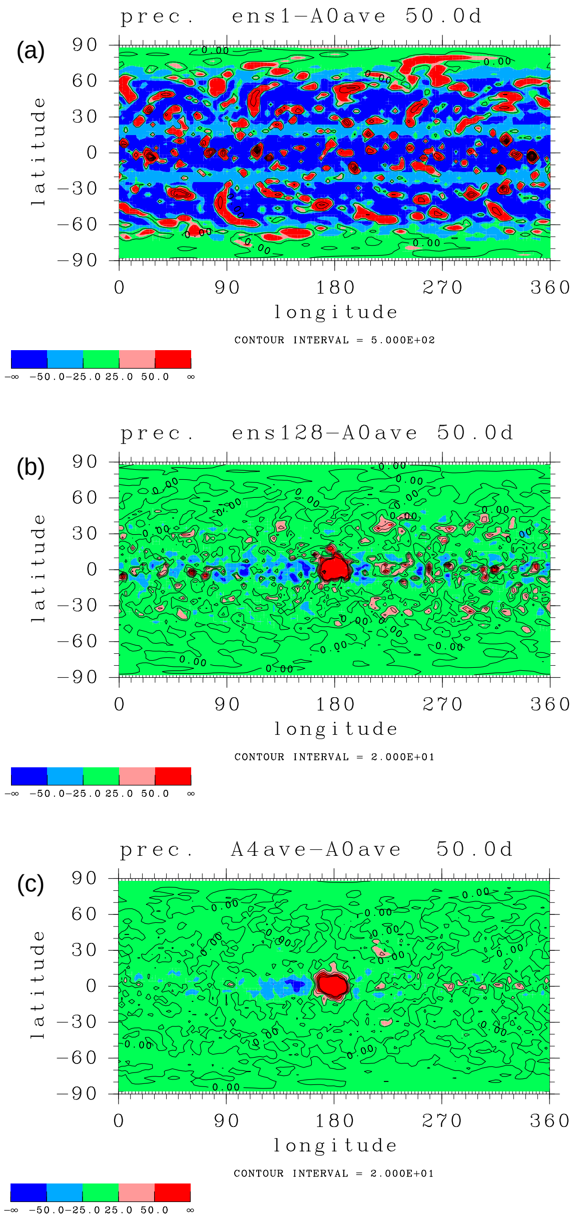

2: Horizontal distribution of precipitation anomaly from zonal and temporal average. (a) at day 50 of 1 run, (b) at day 50 of 128 run mean, and (c) time mean of the long term anomaly experiment. Unit is W/m^2.

Fig.3 (a) and (b) compare the horizontal distributions of the surface pressure anomalies at day 50 of the single run and the 128 ensemble average, respectively. In the result of the single run (Fig.3(a)), little signature of the warm water-related features can be found as in the case of precipitation. In the 128 ensemble mean anomaly field (Fig.3(b)), on the other hand, low pressure area over the warm SST area is quite evident. We can clearly observe an east-west asymmetric pressure response along

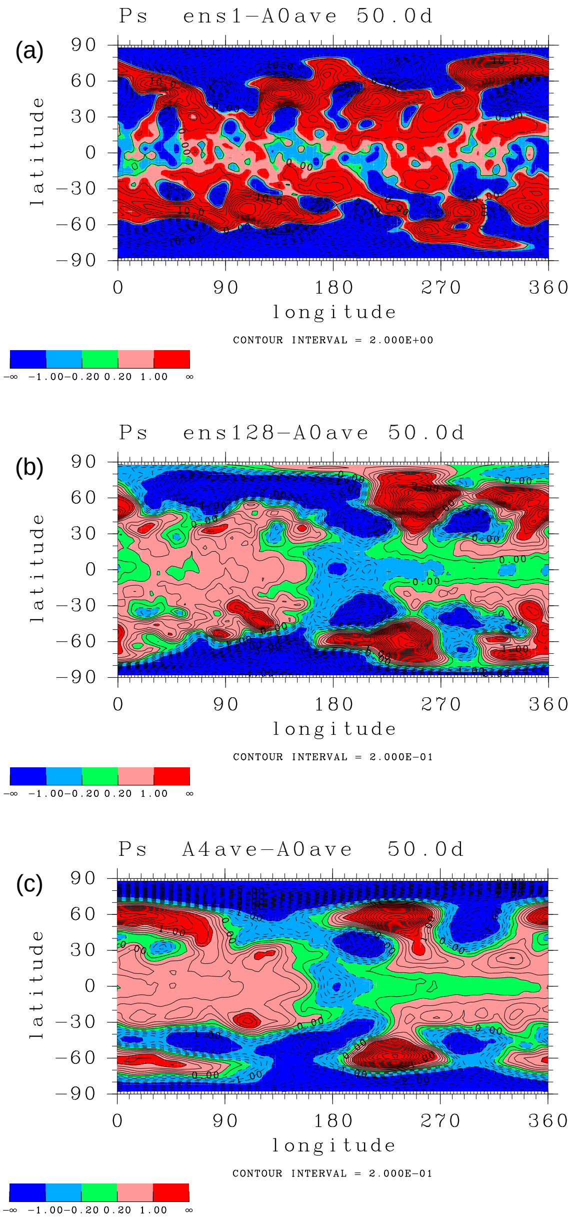

3: Same as Fig.2 but for surface pressure anomaly. Unit is hPa.

the equator. The locations of individual peaks of high or low anomalies also differ between the ensemble and the long time mean anomaly fields. There are two possible causes for those discrepancies. The first is that the number of samples to be averaged is not large enough to eliminate the noise in the extratropical latitudes, and the second, which will be discussed again in the next section, is that the integration duration of each run, 50 days, is not long enough for the establishment of the global steady response.

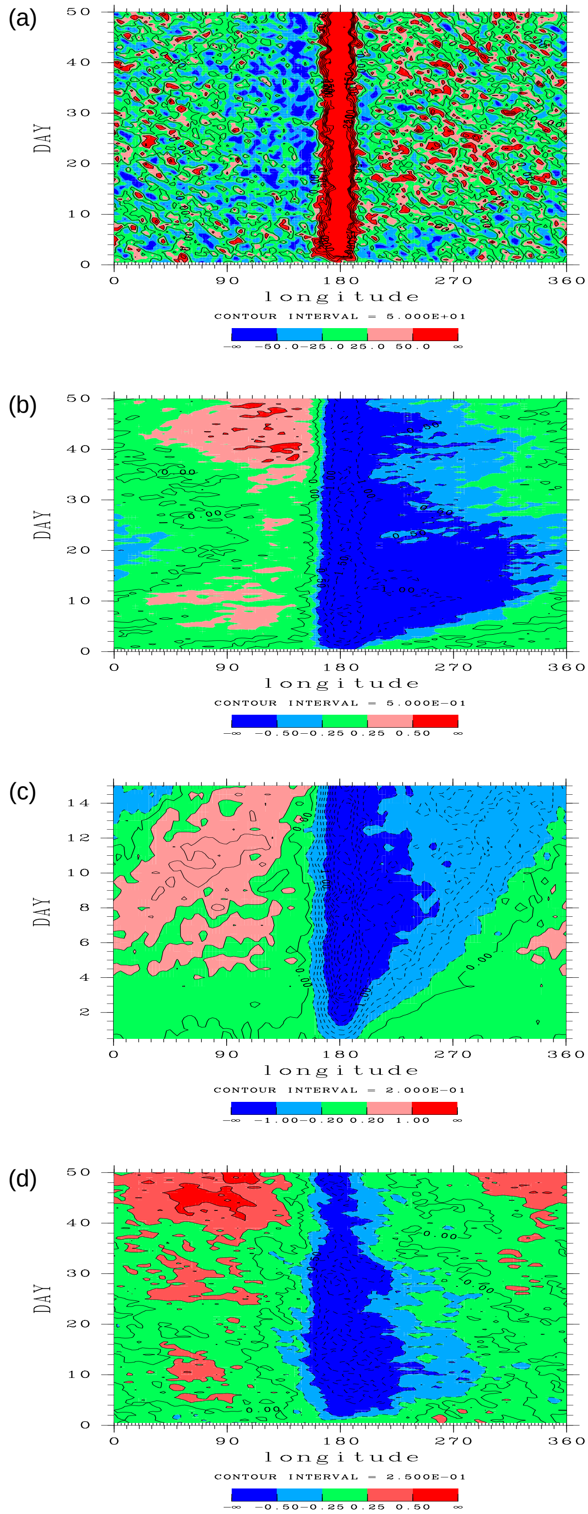

4: Time-longitudinal cross section of ensemble mean anomalies from zonal and temporal average; (a) precipitation (W/m^2) at the equator, (b) surface pressure (hPa) at the equator, (c) same as (b) but the first few days are enhanced, and (d) surface pressure (hPa) at 15°N.

4. DEVELOPMENT OF THE RESPONSE

Fig.4(a) and Fig.4(b) show the time evolutions of the ensemble mean anomalies from zonal and temporal average of precipitation and pressure along the equator, respectively. The response in the first few days is characterized by pressure lowering on and near the area of SST anomaly. This rapid pressure descend is caused by the quick rises of temperature and mixing ratio within the surface boundary layer (not shown here) driven by the sensible and latent heat fluxes from the warm SST anomaly. Increase of precipitation over the warm SST area immediately follows the pressure decrease, although it takes several days for the convection center to be fully established.

Associated with the precipitation increase at the convection center, a widespread pressure rise occurs almost globally. Indeed, Fig.4(c) shows that the pressure rise begins almost simultaneously all over the equatorial circumference. The spread of the response at day 3 is shown in Fig.5, where, except for the low pressure area around the convection center and some signatures of mid latitude Rossby waves, the pressure response is generally positive. Comparison between the surface pressure response and the geopotential response around the tropopause (not shown here) shows that the globally distributed surface high pressure response is associated with the equivalent barotropic vertical structure. This initial pressure rise accounts for about a half of the amount of the high pressure anomaly which appears to the west of the warm SST area in the steady response of H98 and in Fig.3(c).

After this initial response in the first several days, east-west asymmetric features begin to establish. The response to the east of the SST anomaly has a first-baroclinic warm Kelvin wave-like structure; the low pressure anomaly is confined to the region between $\pm 10°$ from the equator and extends eastward. The speed of the eastward extension of the warm Kelvin wave like response is around 20m/s, which is significantly slower than the phase velocity of dry Kelvin wave of the same baroclinic structure ($\sim$ 40 m/s). This slowness implies that the eastern front of the response can be regarded as a "moist" Kelvin wave. In Fig.4(a) it can be recognized that precipitation is suppressed at around the propagating front, which implies that latent heating is positively correlated with vertical velocity. The resulting reduced stability effect (Gill, 1982) explains the slowness of the eastward extension of the response.

The subsequent development, however, deviates from the archetype of the moist Kelvin structure; the precipitation anomaly begins to rebound and becomes positive in a few days after the passage of the response front. With this change of the signature of the precipitation anomaly, the structure of response to the east of the SST anomaly approaches that of H98, which is characterized by a zone of negative pressure and positive precipitation anomaly extending eastward along the equator.

To the west of the SST anomaly, the response in the first several days has a warm Rossby wave characteristics. Although there is no appreciable perturbation along the equator (Fig.4(a)), the pressure perturbation along 15° latitude is negative (Fig.4(d)). The western front is somewhat obscure compared to the eastern moist Kelvin front, but it does propagate westward at the speed of around 6m/s. At the front of the westward response precipitation is slightly suppressed by the downward flow. As is the case with the eastern response front, we can say that the front of the western response is a "moist" Rossby wave. Although the propagation speeds of the fronts are decreased because of the moist reduced gravity effect, the ratio of the speeds of the western and eastern fronts is still about 1:3, which is the ratio of the phase speed Rossby wave to that of Kelvin wave predicted by shallow water equatorial wave theory with long wave approximation (e.g., Matsuno, 1966; Gill 1980).

The precipitation response to the west of the SST anomaly continues to decrease even after the passage of the front. This contrasts to the behavior of precipitation to the east of the SST anomaly, where precipitation rebound occurs after the passage of the front. The mechanism of the continuous decrease of precipitation will be examined later.

Our result shows that the eastward propagation of the moist Kelvin wave front is actually very coherent and long lasting (Fig.4(a)); the moist Kelvin front can be traced encircling the equatorial circumference almost twice. The westward propagation of the moist Rossby wave front, on the other hand, is considerably blurred, and, moreover, pauses around day 15. It seems that the moist Rossby wave extension stops simultaneously with the development of the negative precipitation anomaly to the west of the warm SST area. At around day 15, the precipitation response over the entire tropics develops into the east-west asymmetric distribution; precipitation decrease to the west and increase to the east of the warm SST anomaly along the equator as is reported in H98.

Although the pressure response also establishes to be east-west asymmetric at around day 15, the absolute value of pressure continues to change, since the zon-

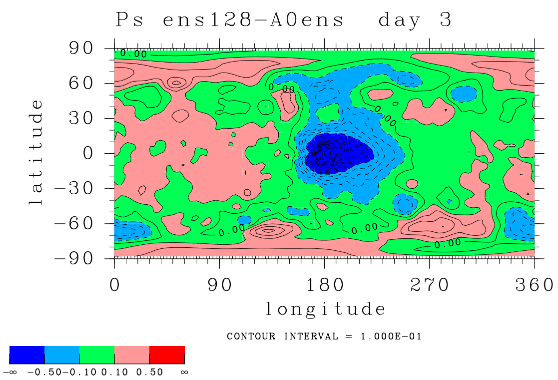

5: Surface pressure ensemble mean anomaly from individual at day 3. Unit is hPa.

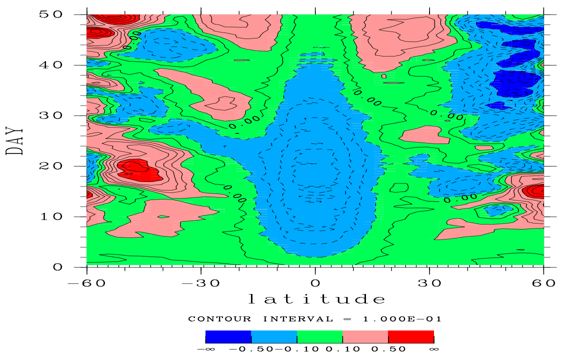

6: Time-latitudinal cross section of zonally averaged ensemble mean surface pressure anomalies from individual. Unit is hPa.

ally symmetric components of the response are still under development. Fig.6 shows time evolution of the zonally averaged surface pressure response. It indicates that pressure in the lower latitudes continues to rise slowly in the later half of the integration period. This tendency of the further increase of equatorial pressure is also expected from the pressure difference between the ensemble mean anomaly at day 50 (Fig.3(b)) and the time mean anomaly (Fig.3(c)). It is probable that another half of the amount of positive pressure anomaly appearing to the west of the warm SST area found in the steady response of H98 is accounted for by this slow mass redistribution between tropical and extratropical latitudes.

5. CAUSES OF THE EAST-WEST ASYMMETRY OF PRECIPITATION

Fig.7 shows the time evolution of the response to the east of the warm SST area averaged zonally in a longitudinal interval from 200° to 267°. In Fig.7(a), it is clearly recognized that the precipitation response at around day 5 is negative, which corresponds to the arrival of the response front as mentioned in the previous section. The rebound of the precipitation anomaly occurs at around day 10, at which time meridional flow in the mixed layer around the latitudes of $\pm 8°$ converging toward the equator develops (Fig.7(b)). The time sequence of the development shown above proves that the increase of precipitation to the east of the warm SST area is caused by the frictional inflow toward the equator where the pressure trough of the moist Kelvin wave develops.

Fig.8 shows the time evolution of the response to the west of the warm SST area averaged zonally in a longitudinal interval from 129° to 158°. At around day 15 in Fig.8(a), the equatorial precipitation anomaly becomes definitely negative. The decrease of precipitation is preceded by the anomalies of meridional flow in the mixed layer along the latitudes of $\pm 10°$ diverging from the equator. The time sequence of the development shown above proves that the decrease of precipitation to the west of the warm SST area is caused by the frictional divergence

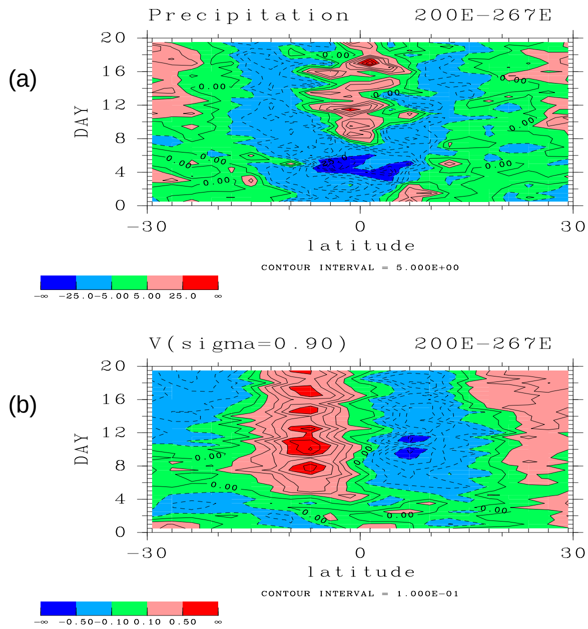

7: Time evolution of the ensemble mean anomaly from zonal and temporal average to the east of the warm SST area averaged zonally in the longitudinal interval from 200° to 267°; (a) precipitation (W/m^2), (b) southerly (m/s) at the lowermost level ($\sigma = 0.995$). Plotted are for the first 20 days.

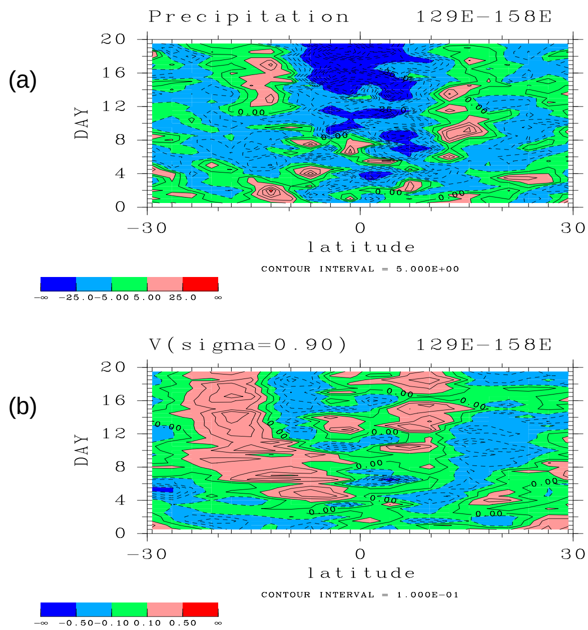

8: Same as Fig.7 but for the ensemble mean anomaly to the west of the warm SST area averaged zonally in the longitudinal interval from 129° to 158°.

of the surface flow from the equator to the longitudes of $\pm 15^\circ$ where the pressure trough of the moist Rossby wave develops.

The characteristics of the structure of responses to the east and to the west of the warm SST area contrast sharply with respect to the signature of the anomalies of precipitation and meridional low level divergence. However, they are governed by the common basic mechanism, i.e., the surface frictional flow divergence/convergence.

6. DISCUSSIONS

Part of the development of the atmospheric response clarified by the present ensemble experiment agrees with the senario of H98. As is expected from the linear theory of Gill(1980), warm Kelvin and warm Rossby wave-like responses associated with the decrease of precipitation develop initially. After several days, precipitation recovers and is even intensified to the east of the warm SST area. To the west of the warm SST area, on the other hand, precipitation decreases monotonically. The east-west asymmetry of the precipitation anomaly is caused by the surface frictional divergence at the equator which is negative (positive) in the Kelvin (Rossby) wave signal emitted to the east (west) of the convection center as is suggested by H98.

The aspects which we have not expected are that a barotropic pressure response appears initially and a zonally symmetric pressure response develops slowly. These two responses explain a considerable amount of high pressure anomaly which remains to the west of the warm SST region in the steady state response.

Another point of importance, which is also a success of ensemble average method, is that the propagation of moist Kelvin wave is clearly identified and that the propagation of the major part of the response occurs in the form of moist Kelvin wave. The noteworthy point is that information on the occurrence of some change extending the full depth of troposphere at the equator tends to propagate eastward not at the speed of dry Kelvin wave, but at the speed of moist Kelvin wave.

The present study have at least two implications concerning the real atmosphere. The first point is that the time scale of the adjustment of the precipitation anomaly, about 15 days, is fairly long compared to the time scale of seasonal variability of the SST or the onset time of ENSO. Second point is the significance of the barotropic response. The existence of the signal associated with barotropic modes in the real atmosphere has been reported, for example, by Hamilton and Garcia (1986) or Matthews and Madden (2000). It must be interesting to examine the relationship between precipitation and global pressure variation using observational data or results of more realistic GCM experiments.

Acknowledgements

The numerical integrations were performed at the supercomputer (NEC SX-4) of the Center for Global Environmental Research, National Institute for Environmental Studies (http://www.nies.go.jp/). The softwares and local computational and information environments were constructed by the use of the resources of GFD-DENNOU CLUB (http://www.gfd-dennou.org/).

Gill, A.E., 1980: Some simple solutions for heat-induced tropical circulation. *Quart. J. Roy. Metor. Soc.*, **106**, 447-462.

Gill, A.E., 1982: Studies of moisture effects in simple atmospheric models: the stable case. *Geophys. Astrophys. Fluid Dynamics*, **19**, 119–152.

Hamilton, K. and R.R. Garcia, 1986: Theory and observations of the Short-period normal mode oscillations of the atmosphere. *J. Geophys. Res.*, **91**, 11867-11875.

Heckley, W.A., and A.E. Gill, 1984: Some simple analytical solutions to the problems of forced equatorial long waves. *Quart. J. Roy. Metor. Soc.*, **110**, 203-217.

Hosaka, M., M. Ishiwatari, S. Takehiro, K. Nakajima, and Y.-Y. Hayashi, 1998: Tropical precipitation patterns in response to a local warm SST area placed at the equator of an aqua planet. *J. Meteor. Soc. Japan*, **76**, 289-305.

Madden, R.A., and P.R. Julian, 1972: Description of global-scale circulation cells in the tropics with a 40-50 day period. *J. Atmos. Sci.*, **29**, 1109-1123.

Matsuno, T., 1966: Quasi-geostrophic motions in the equatorial area. *J. Meteor. Soc. Japan*, **44**, 25-43.

Matthews, A.J., and R.A. Madden, 2000: Observed propagation and structure of the 33-h atmospheric Kelvin wave. *J. Atmos. Sci.*, **57**, 3488-3497.

Toyoda, E., K. Nakajima, M. Ishiwatari, and Y.-Y. Hayashi, 1999: Response of the tropical atmosphere to a localized warm SST area: Time-development observed in an aqua-planet ensemble experiment. *Nagare*, **18**, http://www.nagare.or.jp/mm/99/toyoda/ .

Toyoda, E., K. Nakajima, M. Ishiwatari, S. Takehiro, and Y.-Y. Hayashi, 2002: Tropical precipitation patterns in response to a local warm SST area placed at the equator of an aqua planet: an ensemble study *J. Meteor. Soc. Japan*, submitted.